Styrene Polymerization by Monocyclopentadienyl Titanium(III) Complexes: A DFT Study. The Effect of Counterion on the Kinetics and Mechanism of the Process

Ilya E. Nifant'ev,* Leila Yu. Ustynyuk, and Dmitri V. Besedin

Department of Chemistry, Moscow State University, Moscow 119992, Russia

Received January 27, 2003

The effect of counterion on the kinetics and the mechanism of styrene polymerization by monocyclopentadienyl titanium(III) complexes was examined using the DFT approach. A comparative study of three model catalytic species, namely, $CpTi^{III}CH_2Ph^+$ and two ion pairs of composition $CpTi^{III}CH_2Ph^+A^-$ ($A^- = CH_3B(C_6F_5)_3^-$, $B(C_6F_5)_4^-$), was carried out. Two possible pathways (I and II) of the interaction were examined and compared. It was shown that the nature of the counterion affects the thermodynamic characteristics of styrene addition to the $CpTiCH_2Ph^+A^-$ ion pairs. The weaker the nucleophilicity of the counterion, the higher the exothermicity of styrene addition to $CpTiCH_2Ph^+A^-$. Intramolecular formation of the C−C bond in the $CpTi(CH_2CHPh)CH_2Ph^+A^-$ adduct is characterized by the highest energy on the reaction pathway. This step is the rate-determining stage of the overall reaction.

Introduction

Compounds of type Cp^*TiX_3 (where Cp* is a substituted η^5-C_5H_5 ligand; X = Hal) are known to be efficient catalysts of polymerization of styrene and conjugated dienes.[1−3] Usually, the reactions are carried out with methylalumoxane (MAO) or fluorinated arylboranes as initiators. On the basis of the results of the kinetic, ESR, and NMR studies, Zambelli et al.[4] have first proposed that the active sites are compounds of type $Cp^*Ti^{III}(Pol)^+A^-$, where Pol is the growing polymer chain and A^- is the counterion, e.g., $Me(MAO)^-$ or $MeB(C_6F_5)_3^-$. Complexes of tetravalent[5] and divalent titanium[4−6] were also regarded as the active sites. However, experimental evidence[5,7] showed that tetravalent titanium compounds are inactive in the styrene polymerization reaction owing to steric hindrance for coordination of the styrene molecule imposed by other ligands.

It is nearly generally accepted[8] that for diene polymerization monomer insertion reaction occurs in the same two steps established for olefin polymerization by transition-metal catalytic systems: (i) coordination of the monomer to the metal; (ii) monomer insertion into the metal−carbon bond. This mechanism was studied in detail by modern quantum-chemical methods,[9−16]

* Corresponding author. E-mail: inif@org.chem.msu.ru.

(1) (a) Chien, J. C. W.; Salajka, Z. *J. Polym. Sci., Part A: Polym. Chem.* **1991**, *29*, 1243. (b) Chien, J. C. W.; Salajka, Z. *J. Polym. Sci., Part A: Polym. Chem.* **1991**, *29*, 1253. (c) Foster, P.; Chien, J. C. W.; Rausch, M. D. *Organometallics* **1996**, *15*, 2404.

(2) (a) Kaminsky, W.; Lenk, S. *Macromol. Symp.* **1997**, *118*, 45. (b) Kaminsky, W.; Lenk, S.; Scholz, V.; Roesky, H. W.; Herzog, A. *Macromolecules* **1997**, *30*, 7647.

(3) (a) Schneider, N.; Prosenc, M.-H.; Brintzinger, H.-H. *J. Organomet. Chem.* **1997**, *545*, 291. (b) Xu, G. X.; Ruckenstein, E. *J. Polym. Sci., Part A: Polym. Chem.* **1999**, *37*, 2481. (c) Quyoum, R.; Wang, Q.; Tudoret, M.-J.; Baird, M. C.; Gillis, D. J. *J. Am. Chem. Soc.* **1994**, *116*, 6435.

(4) (a) Grassi, A.; Saccheo, S.; Zambelli, A.; Laschi, F. *Macromolecules* **1998**, *31*, 5588. (b) (a) Grassi, A.; Longo, P.; Proto, A.; Zambelli, A. *Macromolecules* **1989**, *22*, 104. (c) Zambelli, A.; Pellecchia, C.; Oliva, L. *Macromol. Chem., Macromol. Symp.* **1991**, *48/49*, 297. (d) Zambelli, A.; Pellecchia, C.; Oliva, L.; Longo, P.; Grassi, A. *Macromol. Chem.* **1991**, *192*, 223. (e) Longo, P.; Proto, A.; Zambelli, A. *Macromol. Chem. Phys.* **1995**, *196*, 3015. (f) Grassi, A.; Zambelli, A.; Laschi, F. *Organometallics* **1996**, *15*, 480.

(5) Tomotsu, N.; Ishihara, N.; Newman, T. H.; Malanga, M. T. *J. Mol. Catal. A: Chem.* **1998**, *128*, 167.

(6) (a) Kaminsky, W.; Park, Y.-W. *Macromol. Rapid Commun.* **1995**, *16*, 343. (b) Zambelli, A.; Oliva, L.; Pellecchia, C. *Macromolecules* **1989**, *22*, 2129.

(7) Newman, T. H.; Malaga, M. T. *J. Macromol. Sci., Pure Appl. Chem.* **1997**, *34*, 1921.

(8) Costabile, C.; Milano, G.; Cavallo, L.; Guerra, G. *Macromolecules* **2001**, *34*, 7952.

(9) (a) Niu, Sh.; Hall, M. B. *Chem. Rev.* **2000**, *100*, 353. (b) Lauher, J. W.; Hoffmann, R. *J. Am. Chem. Soc.* **1976**, *98*, 1729. (c) Jolly, C. A.; Marynick, D. S. *J. Am. Chem. Soc.* **1989**, *111*, 7968.

(10) (a) Yoshida, T.; Koga, N.; Morokuma, K. *Organometallics* **1995**, *14*, 746. (b) Kawamura-Kuribayashi, H.; Koga, N.; Morokuma, K. *J. Am. Chem. Soc.* **1992**, *114*, 8687. (c) Musaev, D. G.; Froese, R. D. J.; Morokuma, K. *Organometallics* **1998**, *17*, 1850. (d) Vyboishchikov, S. F.; Musaev, D. G.; Froese, R. D. J.; Morokuma, K. *Organometallics* **2001**, *20*, 309.

(11) (a) Fusco, R.; Longo, L.; Masi, F.; Garbassi, F. *Macromolecules* **1997**, *30*, 7673. (b) Fusco, R.; Longo, L.; Provo, A.; Masi, F.; Garbassi, F. *Macromol. Rapid Commun.* **1998**, *19*, 257.

(12) (a) Margl, P.; Deng, L.; Ziegler, T. *Organometallics* **1998**, *17*, 933. (b) Margl, P.; Lohrenz, J. C. W.; Ziegler, T.; Blöchl P. *J. Am. Chem. Soc.* **1996**, *118*, 4434. (c) Lohrenz, J. C. W.; Woo, T. K.; Ziegler, T. *J. Am. Chem. Soc.* **1995**, *117*, 2793. (d) Woo, T. K.; Fan, L.; Ziegler, T. *Organometallics* **1994**, *13*, 2252. (e) Lohrenz, J. C. W.; Woo, T. K.; Fan, L.; Ziegler, T. *J. Organomet. Chem.* **1995**, *497*, 91.

(13) (a) Chan, M. S. W.; Vanka, K.; Pye, C. C.; Ziegler, T. *Organometallics* **1999**, *18*, 4624. (b) Vanka, K.; Chan, M. S. W.; Pye, C. C.; Ziegler, T. *Organometallics* **2000**, *10*, 1841. (c) Chan, M. S. W.; Ziegler, T. *Organometallics* **2000**, *24*, 5182.

(14) (a) Lanza, G.; Fragala, I. L.; Marks, T. J. *J. Am. Chem. Soc.* **1998**, *120*, 8257. (b) Lanza, G.; Fragala, I. L.; Marks, T. J. *J. Am. Chem. Soc.* **2000**, *122*, 12764. (c) Lanza, G.; Fragala, I. L.; Marks, T. J. *Organometallics* **2002**, *21*, 5594.

(15) Lieber, S.; Prosenc, M.-H.; Brintzinger, H.-H. *Organometallics* **2000**, *19*, 377.

(16) (a) Støvneng, J. A.; Rytter, E. *J. Organomet. Chem.* **1996**, *519*, 277. (b) Thorshang, K.; Støvneng, J. A.; Rytter, E.; Ystenes, M. *Macromolecules* **1998**, *31*, 7149. (c) Thorshang, K.; Støvneng, J. A.; Rytter, E. *Macromolecules* **2000**, *33*, 8136.

10.1021/om0300629 CCC: $25.00
Publication on Web 05/29/2003

whereas the polymerization of styrene and conjugated dienes on monocyclopentadienyl titanium compounds has attracted increasing attention of quantum chemists only recently.

Corradini and Cavallo et al.[8,17,18] have contributed largely to the development of this research avenue. They studied[18] the mechanisms of the interaction between the model compounds $CpTi^{III}(Pol)^+$ and $CpTi^{II}(Pol)$ and the styrene molecule using the DFT approach and found that Ti(II) compounds must be much less active than the corresponding Ti(III) compounds. Because of this, we leave the divalent titanium compounds out of consideration.

The major drawback of the studies of the mechanism of olefin polymerization by metallocene catalysts is the use of a simple cationic model of the catalyst (no counterion was considered). Earlier, the effect of the counterion on the energy profile of the polymerization reaction was studied by Ziegler et al.[13] and Marks et al.[14] Recently[19] we have studied the dependence of the energy profile of the reaction $Cp_2ZrEt^+A^- + C_2H_4 \rightarrow Cp_2ZrBu^+A^-$ on the "nucleophilicity" of the counterion A^-. We revealed that the energy profiles of the reactions of ethylene with isolated cation and with ion pairs are significantly different and found that the enhancement of the nucleophilicity of the counterion can also be responsible for qualitative changes in the reaction mechanism.

In this work we report a comparative study of the mechanisms and energy profiles of the model reactions $CpTi^{III}R^+A^-$ + styrene (R = benzyl) and of their dependence on the nature of the counterion.

Computational Details

All calculations were carried out using the original program PRIRODA developed by D. N. Laikov.[20] The generalized gradient approximation (GGA) for the exchange−correlation functional by Perdew, Burke, and Ernzerhof[21] was employed. The 10 core electrons of Ti and 2 for B, C, O, and F were described by effective core potentials.[22] The orbital basis sets of contracted Gaussian-type functions of size (5s1p)/[3s1p] for H, (5s5p2d)/[3s3p2d] for B, C, O, and F, and (9s9p8d)/[5s5p4d] for Ti were used for the remaining electrons in conjunction with the density-fitting basis sets of uncontracted Gaussian-type functions of size (5s1p) for H, (6s3p3d1f) for B, C, O, and F and (10s6p6d5f5g) for Ti. The spin-unrestricted DFT method was used for open-shell species.

Full optimization of the geometry of the structures studied in this work was performed using analytical gradients and followed by analytical calculations of the second derivatives of energy with respect to coordinates in order to characterize the nature of the resulting stationary points (minima or saddle points) on the potential energy surface (PES). Vibrational frequencies, zero-point vibrational energies, and thermodynamic data were calculated using ideal gas, rigid rotor, and harmonic oscillator approximations.

Results and Discussion

The Isomers of $CpTiCH_2Ph^+A^-$. The $CpTiCH_2Ph^+$ cation is the simplest model of the catalytic species. We performed a thorough study of the interaction between this specimen and the styrene molecule and revealed the key intermediates and transition states (TS) on the reaction pathway. Despite the fact that this system has already been studied by Cavallo et al.,[18] it is appropriate to reconsider it because the results of our calculations appeared to be somewhat different from the published data.

Three energy minima corresponding to three isomers (**1a**, **2a**, and **3a**) were located on the potential energy surface of the $CpTiCH_2Ph^+$ system. The isomers are characterized by different hapticity of coordination of the benzyl fragment, namely, η^7 (**1a**), η^3 (**2a**), and η^1 (**3a**). The structures of **1a**, **2a**, and **3a** are presented in Figure 1, and selected geometric parameters are listed in Table 1. Of the three structures found in this work, two (**1a** and **3a**) were considered by Cavallo et al. (structures *1c* and *1d*, respectively, in ref 18a). As can be seen from the data listed in Table 1, the geometric parameters of the $CpTiCH_2Ph^+$ system obtained by Cavallo et al.[18] and from our calculations are close.

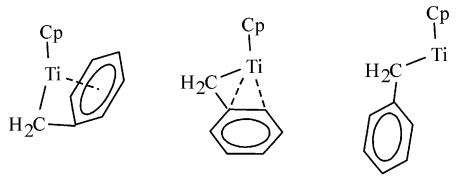

1a **2a** **3a**

In the presence of the counterion A^- (the structures with the $B(C_6F_5)_4^-$ and $CH_3B(C_6F_5)_3^-$ anions are respectively labeled **b** and **c**) the hapticity of coordination of the benzyl fragments in the complexes **1b**,**c** and **2b**,**c** is the same as that in the cationic complexes **1a** and **2a**, respectively. This is indicated by the distances from the Ti atom to the carbon atoms C_1-C_7 (see Table 1). The appearance of the counterion A^- leads to the formation of two isomers similar to **2a** and having the same hapticity (η^3). Complexes **2b**,**c** and **2′b**,**c** (Figure 2, Table 1) differ in orientation of the benzyl ligand relative to the CpTi "core"; in other words, the Ph group of the benzyl fragment can be directed either "upward" (toward the Cp ring) or "downward" (in the opposite direction). The energy difference between **2b**,**c** and **2′b**,**c** is tiny (at most 0.7 kcal mol^{-1}). The most thermodynamically stable complexes are **2′b** for $A^- = B(C_6F_5)_4^-$ and **2c** for $A^- = CH_3B(C_6F_5)_3^-$. In this work we considered two channels of the reaction ($CpTiCH_2Ph^+A^-$ + styrene) using the complexes **2b**,**c** and **2′b**,**c** as the resting state of the model catalytic species $CpTiCH_2Ph^+A^-$. All attempts to optimize the geometry of η^1-complexes **3b**,**c** led to the isomers **2b**,**c** or **2′b**,**c**, which suggests that the structures **3b**,**c** do not exist.

As we have shown earlier in the study of the $Cp_2ZrEt^+A^-$ ion pairs with the same counterions,[19] the

(17) (a) Cavallo, L.; Guerra, G.; Corradini, P. *J. Am. Chem. Soc.* **1998**, *120*, 2428. (b) Cavallo, L.; Guerra, G. *Macromolecules* **1996**, *29*, 2729.

(18) (a) Minieri, G.; Corradini, P.; Zambelli, A.; Guerra, G.; Cavallo, L. *Macromolecules* **2001**, *34*, 2459. (b) Minieri, G.; Corradini, P.; Zambelli, A.; Guerra, G.; Cavallo, L. *Macromolecules* **2001**, *34*, 5379.

(19) (a) Nifant'ev, I. E.; Ustynyuk, L. Yu.; Laikov, D. N. In *Organometallic Catayst and Olefin Polymerization*; Blom, R., Follestad, A., Rytter, E., Tilset, M., Ystenes, M., Eds.; Springer-Verlag: Berlin, 2001; p 72. (b) Nifant'ev, I. E.; Ustynyuk, L. Yu.; Laikov, D. N. *Organometallics* **2001**, *20*, 5375.

(20) Laikov, D. N. *Chem. Phys. Lett.* **1997**, *281*, 151.

(21) Perdew, J. P.; Burke, K.; Ernzerhof, M. *Phys. Rev. Lett.* **1996**, *77*, 3865.

(22) (a) Stevens, W. J.; Basch, H.; Krauss, M. *J. Chem. Phys.* **1984**, *81*, 6026. (b) Stevens, W. J.; Basch, H.; Krauss, M.; Jasien, P. *Can. J. Chem.* **1992**, *70*, 612. (c) Cundari, T. R.; Stevens, W. J. *J. Chem. Phys.* **1993**, *98*, 5555.

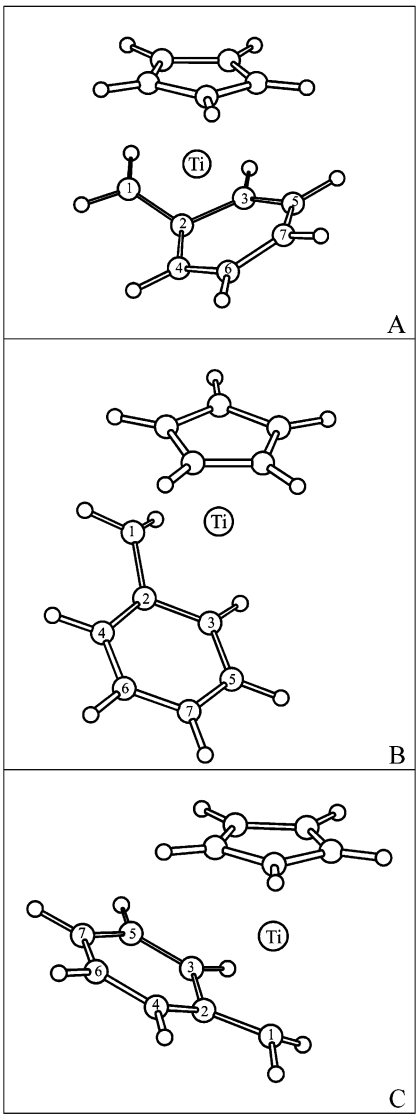

Figure 1. Structures of complexes **1a** (A), **2a** (B), and **3a** (C).

H and F atoms of the anion can interact with the metal ion, thus filling the coordination vacancy and stabilizing the corresponding structure. Several experimental observations (first of all, by X-ray diffraction analysis; see, e.g., ref 23) of this type of interaction have been reported. Complex **2b** (**2′b**) exhibits two short Ti−F contacts of length 2.27 and 2.30 Å (2.26 and 2.30 Å) with the atoms of the C_6F_5 fragment of the corresponding anion (Table 1).

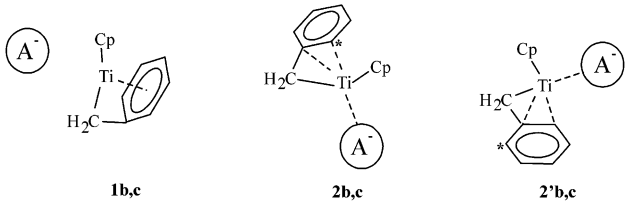

No Ti−F contacts occur in the structure of complex **1b** (all Ti−F distances are longer than 3.76 Å).[24] This can be rationalized as follows. First, the C_1−C_7 atoms in **1b** fill the coordination vacancy of the Ti atom. Second, the distance from the central ion to the bulky $B(C_6F_5)_4^-$ anion in **1b** is longer than in the complexes **2b** and **2′b** characterized by lower hapticity of coordination of the benzyl fragment. This is also indicated by the longer Ti−B distance in **1b** compared to **2b** and **2′b** (5.90 vs 5.25 and 5.45 Å, respectively).

Complexes **1c**, **2c**, and **2′c** correspondingly exhibit one, three, and three short Ti−H contacts (2.1−2.4 Å) with the hydrogen atoms of the bridging CH_3 group. The Ti−B and Ti−C distances in **1c** are much longer than in **2c** and **2′c** (4.31 vs 3.94 and 3.95 Å and 2.72 vs 2.27 and 2.27 Å, respectively). Complex **1b** is characterized by the absence of short contacts between the Ti atom and the atoms of the counterion. Contrary, complex **1c** exhibits one short Ti−H contact (2.21 Å), which seems to be due to the fact that the $CH_3B(C_6F_5)_3^-$ anion is smaller than the $B(C_6F_5)_4^-$ anion.

Comparison of the energy characteristics of complexes **1a**−**c** and **2a**−**c**/**2′a**−**c** (Table 2) suggests that the energy difference between **1a**−**c** and **2a**−**c**/**2′a**−**c** is appreciably different for the cation (**a**) and for the ion pairs (**b**, **c**). In the case of the $CpTiCH_2Ph^+$ cation, complex **1a** has a lower energy compared to **2a**. In the case of the ion pairs, the energies of complexes **2b**/**2′b** and **2c**/**2′c** are lower than those of **1b** and **1c**, respectively. Such an inversion of the energy difference between **1b**,**c** and **2b**,**c**/**2′b**,**c** in the latter case is associated with the stabilization of **2b**,**c**/**2′b**,**c** due to the interaction with the counterion.

Interaction of Styrene with $CpTiCH_2Ph^+A^-$. I. Key Intermediates and Transition States on the Reaction Pathway. The interaction of isolated $CpTiCH_2Ph^+$ cation (a) with the styrene molecule has been studied in detail by Cavallo et al.,[18] who considered the η^7-complex **1a** as the resting state of the catalyst. They also showed[18] that the reaction involves the formation of intermediates and TS characterized by different hapticity of coordination of the benzyl fragment (η^3) compared to the initial complex **1a**. In the case of the ion pairs, the η^3-complexes **2b**,**c**/**2′b**,**c** have lower energies compared to **1b**,**c**, and that results in Pathway I (Scheme 1), which treats the η^3-complexes **2a**−**c**/**2′a**−**c** as the resting state of the catalyst.

In this work, we succeeded in reproducing the geometries and energies of the key intermediate (**4a** in this work and *2e* in ref 18a) and TS (**5a** in this work and *3c* in ref 18a) of Pathway I (P-I) with high accuracy and suggest yet another reaction channel (Pathway II (P-II), Scheme 2), which is characterized by similar energy profiles for all the systems studied. The major difference between P-I and P-II is as follows: the reaction proceeds by P-I if the isomers **2′a**−**c** act as an initial complex; P-II is realized when complexes **2a**−**c** are the resting state. In the case of the isolated cation, the structures **2a** and **2′a** are degenerate. Barrierless styrene addition to **2a** proceeds by P-I and P-II following two different channels. Both mechanisms involve the intermediates and TS with a η^3-coordinated benzyl ligand. Let us consider them in more detail.

(23) (a) Yang, X.; Stern, Ch. L.; Marks, T. J. *J. Am. Chem. Soc.* **1994**, *116*, 10015. (b) Jia, L.; Yang, X.; Stern, Ch. L.; Marks, T. J. *Organometallics* **1997**, *16*, 842. (c) Karl, J.; Erker, G.; Frohlich, R. *J. Am. Chem. Soc.* **1997**, *119*, 11165.

(24) Figures of the structures **1b**,**c**, **4b**,**c**, **5b**,**c**, **7b**,**c**, **8b**,**c**, **9b**,**c**, **10b**,**c**, **12b**,**c**, **13b**,**c**, **14c**, **15c**, **17c**, **18c**, **16b**,**c**, **16′b**,**c**, and **19b**,**c** are available as Supporting Information.

Table 1. Selected Distances (Å) in Isomers of Model Compounds $CpTiCH_2Ph^+A^-$

	Ti−C_1[a]			Ti−C_{2-7}[b]				Ti−B	Ti−F[c]		Ti−C[c]		Ti−H[c]	
1a	2.54	2.18	2.34	2.33	2.44	2.41	2.39							
1a[d]	2.60	2.19	2.35	2.34	2.46	2.44	2.40							
1b	2.55	2.18	2.33	2.33	2.43	2.42	2.39	5.90	3.76	4.04				
1c	2.58	2.21	2.33	2.40	2.44	2.49	2.43	4.31			2.72	2.21	2.69	2.95
2a	2.16	2.32	2.29	3.29	3.25	4.00	3.98							
2b	2.17	2.38	2.38	3.44	3.45	4.23	4.24	5.25	2.27	2.30				
2′b	2.20	2.33	2.56	3.08	3.48	3.88	4.06	5.45	2.26	2.30				
2c	2.18	2.40	2.39	3.45	3.46	4.24	4.25	3.94			2.27	2.13	2.13	2.39
2′c	2.19	2.37	2.47	3.30	3.46	4.08	4.15	3.95			2.27	2.14	2.18	2.33
3a	2.14	2.25	2.74	2.73	3.61	3.60	3.99							
3a[d]	2.14	2.27	2.80	2.72	3.66	3.60	4.01							

[a] The atomic numbering scheme is shown in Figures 1 and 2. [b] Carbon atoms of the Ph group. [c] Bridging atoms of the CH_3 and C_6F_5 fragments of the anion A^-. [d] Obtained by Cavallo et al.[18a] for structures *1c* and *1d* (analogues of structures **1a** and **3a** in this work, respectively).

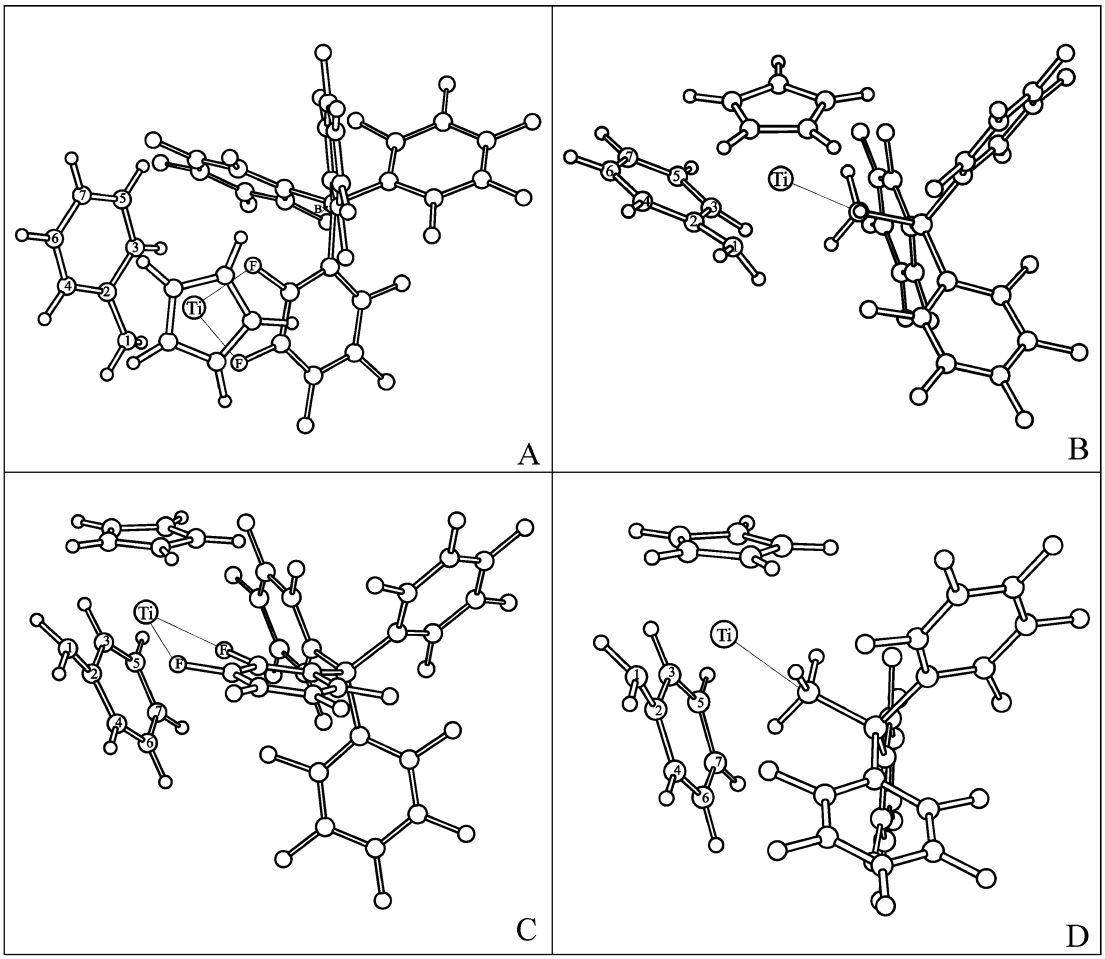

Figure 2. Structures of complexes **2b** (A), **2c** (B), **2′b** (C), and **2′c** (D).

Table 2. Thermodynamic Characteristics of Isomers of the Model Compounds $CpTiCH_2Ph^+A^-$ Relative to Isomers 2 (2a, 2b, and 2c, if no counterion is involved (a), $B(C_6F_5)_4^-$ (b), or $CH_3B(C_6F_5)_3^-$ (c))

characteristic[a]	**1a**	**3a**	**1b**	**2′b**	**1c**	**2′c**
ΔE, kcal mol^{-1}	−13.3	0.5	2.3	−0.7	1.0	0.7
ΔH_0, kcal mol^{-1}	−12.7	0.5	2.7	−0.4	2.0	0.9
ΔH_{298}, kcal mol^{-1}	−12.9	0.6	2.9	−0.2	1.8	0.9
ΔG_{298}, kcal mol^{-1}	−11.9	0.3	−0.5	−1.0	4.7	2.4

[a] The corresponding characteristics of isomers **2** were set to zero.

I.a. $CpTiCH_2Ph^+$ Cation (a). In P-I, the key role is played by the intermediate **4a** (*2e* in ref 18a) and TS **5a** (*3c* in ref 18a). Their geometries are presented in Figure 3; the selected distances are listed in Table 3. The highest energy barrier on P-I corresponds to the formation of the C−C bond in intermediate **4a** via TS **5a**. This transformation results in the primary γ-agostic product **6a** (*4a* in ref 18a).

In the framework of the P-II the interaction of the styrene molecule with the cationic complex immediately results in the pre-reaction complex **7a** (Figure 4, Table 3). Styrene addition to **2a** resulting in **7a** (and an analogous process resulting in **4a**) occurs barrierlessly and is accompanied by substantial decrease in the energy of the system. Further transformation of **7a** via TS **8a** results in a thermodynamically stable product

Scheme 1. Pathway I

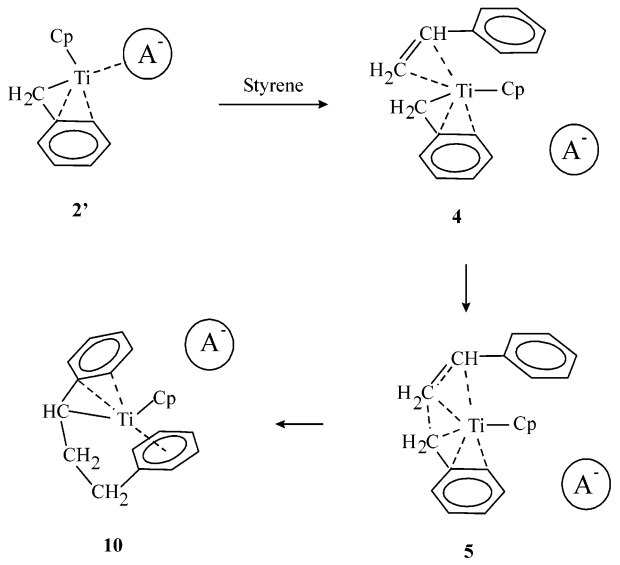

Scheme 2. Pathway II

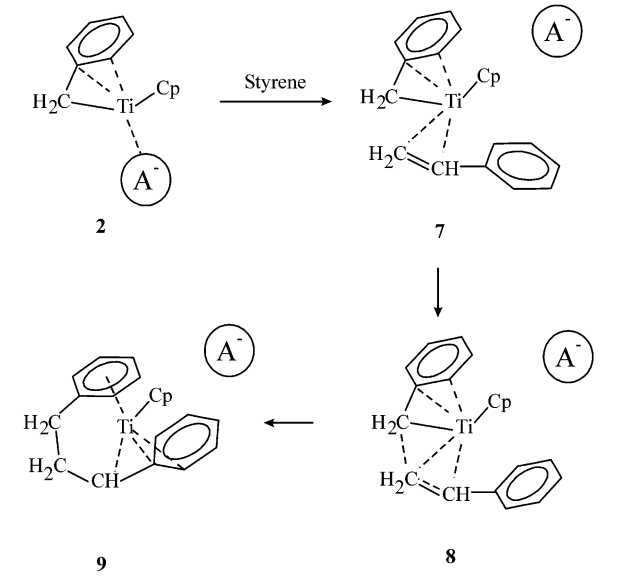

9a bypassing the stage of formation of the kinetic product (an analogue of **6a** for the above-mentioned case).

Let us consider in detail the key features and differences between the P-I and P-II taking the isolated cation case (**a**) as an example. First of all, they differ in the manner of coordination of the styrene molecule, which in this work is denoted as the *cis*-like coordination (the C_8 atom of the styrene molecule is headed toward the C_{11} atom) and the *trans*-like coordination. If P-I is realized, the *cis*-like coordination is retained in the intermediate **4a**, in TS **5a**, and in the kinetic product **6a** (Figure 3, Table 3). In the case of P-II, the *trans*-like coordination of the styrene fragment in the intermediate **7a** changes into the *cis*-like coordination in TS **8a** and the product **9a** (Figure 4, Table 3). Second, a feature of TS **5a** is the α-agostic bond with one of the two hydrogen atoms at the C_1 atom. The corresponding Ti−H distance is 2.28 Å and the C_1−H bond is 0.01 Å longer than the conventional C−H bond (1.11 vs 1.10 Å, respectively). No Ti−H agostic interactions occur in TS **8a**. Third, the kinetic products **6a** and **9a** have fundamentally different geometries. Relaxation of TS **5a** results in the insertion product **6a**, in which the coordination vacancy is filled due to η^2-coordination of the terminal Ph group (the corresponding Ti−C distances are 2.57 and 2.65 Å), on one hand, and the formation of the Ti−H agostic bond with one hydrogen atom at the C_1 atom, on the other hand. The corresponding Ti−H distance is 2.27 Å, while the C_1−H bond length is 1.12 Å. Thus, the α-agostic bond in TS **5a** turns into the γ-agostic bond in product **6a**. In complex **9a** the coordination vacancy of Ti is filled due to η^6-coordination of the terminal Ph group. This is indicated by the distances from the Ti atom to the C_2−C_7 atoms (2.45, 2.42, 2.49, 2.51, 2.52, and 2.52 Å, respectively). Compound **9a** is 13.4 kcal mol^{-1} more stable than **6a**.

It is important to note that the geometric parameters of structures **4a** and **5a** in this work and their analogues in ref 18a (*2e* and *3c*, respectively) coincide (Table 3). However, in the case of product **6a** they are somewhat different from those obtained in ref 18a (*4a*), though the key structural features match (Table 3).

In addition, complex **6a** is a thermodynamically unstable product. It can undergo a facile isomerization by the γ-agostic bond cleavage, which results in complex **10a** with η^6-coordination of the terminal Ph group (Figure 3, Table 3). The structure and energy characteristics of **10a** and **9a** are close. Further transformations of the reaction products **9a** and **10a** will be considered below.

Thus, the energy profiles (Table 4) obtained for P-I and P-II are similar, which suggests the existence of two reaction channels. In this connection, it is of particular importance to answer the question as to how the presence of the counterion can affect the energy profile of the reaction.

I.b. $CpTiCH_2Ph^+A^-$ Ion Pairs (b and c). For the $CpTiCH_2Ph^+A^-$ ion pairs (**b** and **c**) we optimized the structures of intermediates **4b**,**c** and **7b**,**c**, TS **5b**,**c** and **8b**,**c**, and the primary reaction products **10b**,**c** and **9b**,**c** (Tables 3 and 4) for the two pathways (P-I and P-II) of interaction of the isomers **2′b**,**c** and **2b**,**c** with the styrene molecule, which were considered above taking the $CpTiCH_2Ph^+$ cation as an example. In contrast to the reaction with the cation, we failed to locate the γ-agostic products **6b**,**c** on the potential energy surface of the system; that is, the relaxation of the TS **5b** and **5c** immediately leads to **10b** and **10c**, respectively, bypassing the stage of formation of the corresponding intermediates **6b** and **6c**.[24]

In both cases, **b** and **c**, the Ti−B distances in the intermediates **7b**,**c** and TS **8b**,**c** are shorter than those in the intermediates **4b**,**c** and TS **5b**,**c**, respectively. This distance is somewhat shortened as the system moves from the intermediates to the products, while all other geometric parameters of structures **4b**,**c**−**10b**,**c** are close to those found for **4a**−**10a** (see section I.a). The cation−anion interaction causes some changes in the energy profiles for P-I and P-II involving the ion pairs **b** and **c** compared to the energy profile of the reaction with the isolated cation (**a**). The appearance of the counterion and an enhancement of its nucleophilicity (if we pass from **b** to **c**) lead to a decrease in the exothermicity of the addition of the styrene molecule

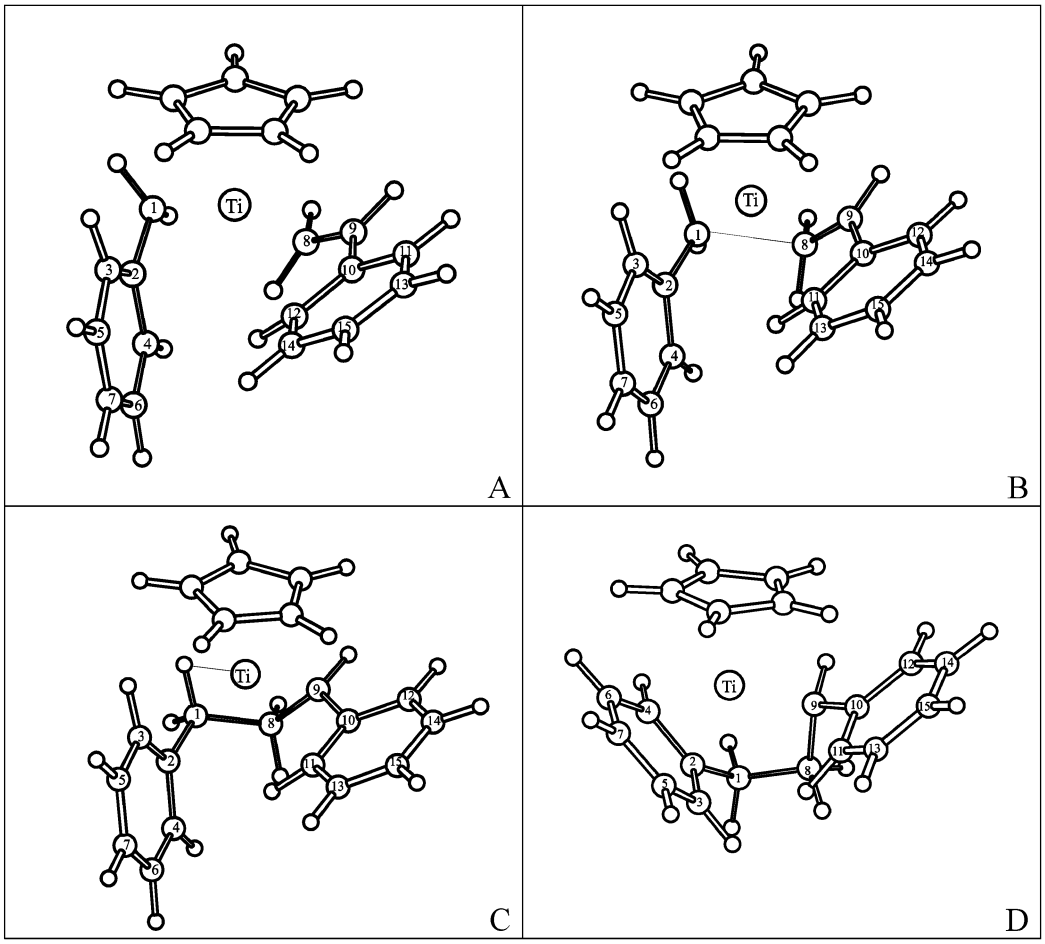

Figure 3. Structures of the intermediate **4a** (A), TS **5a** (B), primary **6a** (C), and secondary **10a** (D) products for Pathway I.

Table 3. Selected Distances (in Å) in Complexes and Transition States 6−10 with η^3-Coordinated Benzyl Fragment

	styrene coordination type	Ti−C_1[a]	Ti−C_{2-3}[a]		Ti−C_{8-11}[a]				C_1-C_8[a]	Ti−B
4a (*2e*)	*cis*	2.24 (2.23)[b]	2.47 (2.48)	2.67 (2.65)	2.38 (2.38)	2.40 (2.39)	2.53 (2.54)	2.51 (2.59)	2.92	
5a (*3c*)	*cis*	2.28 (2.29)[b]	2.57 (2.57)	2.59 (2.58)	2.45 (2.48)	2.22 (2.22)	2.43 (2.44)	2.43 (2.45)	2.12 (2.12)	
6a (*4a*)	*cis*	2.51 (3.33)[b]	2.65 (2.88)	2.57 (2.42)	2.64 (3.15)	2.14 (2.21)	2.38 (2.33)	2.40 (2.35)	1.59 (1.54)	
10a	*cis*	3.43	2.47	2.52	3.28	2.30	2.63	2.72	1.54	
7a	*trans*	2.18	2.46	2.47	2.51	2.33	2.54	2.96	3.15	
8a	*cis*	2.43	2.36	2.60	2.49	2.21	2.50	2.56	2.07	
9a	*cis*	3.31	2.45	2.52	3.40	2.31	2.62	2.76	1.54	
4b	*cis*	2.24	2.47	2.67	2.38	2.40	2.53	2.51	2.91	7.03
5b	*cis*	2.28	2.59	2.61	2.44	2.22	2.43	2.42	2.10	7.05
10b	*cis*	3.43	2.47	2.52	3.28	2.30	2.64	2.72	1.54	6.67
7b	*trans*	2.19	2.46	2.46	2.50	2.34	2.55	2.97	3.14	6.99
8b	*cis*	2.43	2.37	2.60	2.49	2.21	2.52	2.60	2.07	7.01
9b	*cis*	3.39	2.44	2.52	3.31	2.31	2.63	2.77	1.54	6.63
4c	*cis*	2.23	2.49	2.64	2.38	2.40	2.54	2.55	2.93	6.54
5c	*cis*	2.29	2.59	2.59	2.45	2.21	2.42	2.43	2.09	6.39
10c	*cis*	3.43	2.47	2.53	3.28	2.30	2.63	2.71	1.54	6.05
7c	*trans*	2.19	2.46	2.47	2.50	2.33	2.58	3.04	3.14	6.31
8c	*cis*	2.43	2.38	2.61	2.49	2.21	2.53	2.62	2.07	6.22
9c	*cis*	3.39	2.45	2.45	3.30	2.30	2.63	2.79	1.54	6.05

[a] The atomic numbering scheme is shown in Figures 3 and 4. [b] Obtained by Cavallo et al.[18a] for structures *2e*, *3c*, and *4a* (analogues of structures **4a**, **5a**, and **6a** in this work, respectively).

to complexes **2a**−**c** and, as a consequence, to a decrease in the total energy effect of the reaction (Table 4). Analogous changes in the energy profile were also reported in our earlier study[19] of the interaction between the $Cp_2ZrEt^+A^-$ ion pairs and the ethylene molecule carried out with the same counterions.

Thus, we have shown that there are at least two reaction channels characterized by close energies of the intermediates and TS. One of the mechanisms was earlier proposed by Cavallo et al.,[18] who considered the η^7-complex **1a** (*1c* in ref 18a) as the resting state of the catalyst. As it was mentioned and substantiated above,

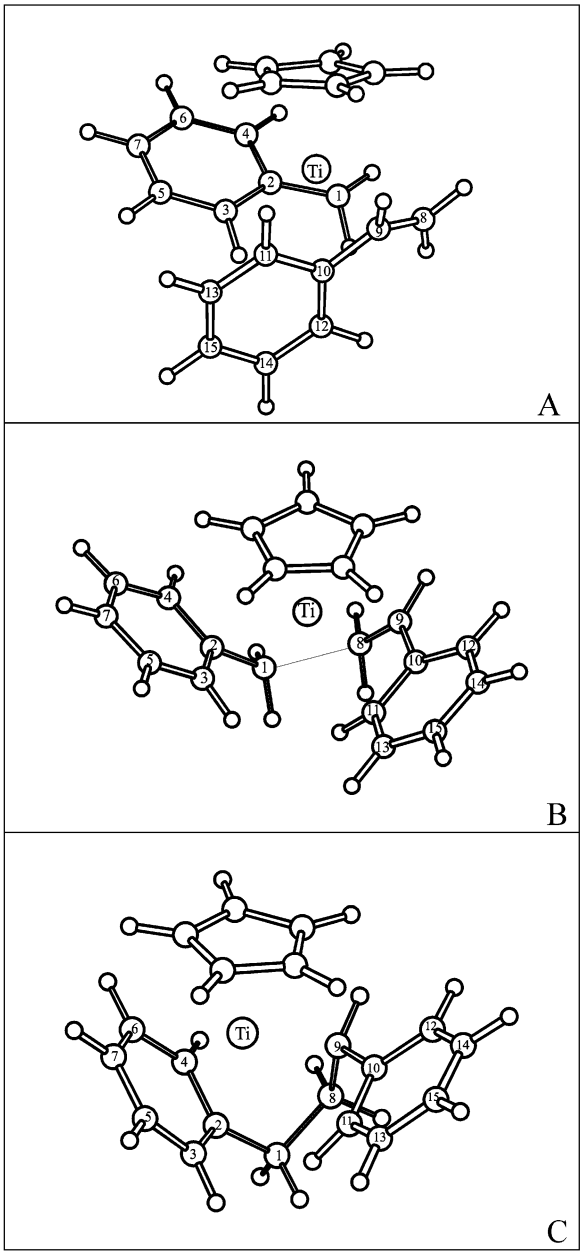

Figure 4. Structures of the intermediate **7a** (A), TS **8a** (B), and product **9a** (C) for Pathway II.

in this work we treat the η^3-complex **2a** as the resting state. This assumption requires only a modification of the reaction pathway rather than a revision of the entire mechanism.

The energy profiles obtained for P-I and P-II are similar for all three cases (**a**, **b**, and **c**); that is, a change in the reaction channel causes no pronounced variations of both the kinetic and thermodynamic characteristics of the reactions under study.

II. Mechanism and the Energy Profile of Styrene Addition to the $CpTiCH_2Ph^+A^-$ Ion Pairs with the Formation of $CpTi(CH_2CHPh)CH_2Ph^+A^-$ Adducts (4 and 7). Earlier,[19] we showed that, contrary to the reaction with the isolated cation, ethylene addition to the model catalytic species $Cp_2ZrEt^+A^-$ in the presence of a counterion to give an intermediate complex $Cp_2Zr(C_2H_4)Et^+A^-$ does not occur barrierlessly. The energy barrier arises due to the necessity of displacing the counterion by the substrate from the coordination sphere of Zr; therefore, this barrier is maximal for the most nucleophilic counterion, $CH_3B(C_6F_5)_3^-$. Since the mechanisms of ethylene addition to $Cp_2ZrEt^+A^-$ and of styrene addition to $CpTiCH_2Ph^+A^-$ follow in some sense the same pattern, one should expect that the substrate addition in the latter case also would not occur barrierlessly. This gives us an impetus to a more detailed consideration of the styrene addition to the $CpTiCH_2Ph^+A^-$ ion pair taking complexes **2a**−**c** as an example.

In contrast to the reaction with cation **2a**, styrene addition to the model compound **2c** to form the pre-reaction complex **7c** involves two stages and requires the overcoming of two energy barriers (Scheme 3). At the first stage, styrene addition to **2c** occurs to form the intermediate complex **11c**. The energy barrier (**12c**) to this reaction is low (Table 5). The benzyl fragment and the styrene molecule in complex **11c** are coordinated in a η^1- and η^2-manner, respectively, and the distance to the carbon atom of the bridging CH_3 group (2.54 Å) is slightly longer than the corresponding distance in **2c** (2.37 Å). The addition of the styrene molecule to **2c** leads to a decrease in energy (however, to a lesser extent compared to the addition to **2a**) (Table 5).

Further transformation of **11c** into the pre-reaction complex **7c** via TS **13c** leads to a substantial increase in the energy of the system and occurs by rotating the styrene molecule in the coordination sphere of Ti with simultaneous lengthening of the Ti−B and Ti−C distances to the bridging CH_3 group. The energy of TS **13c** is nearly 6.0 kcal mol^{-1}, which is higher than the energy barrier to the first reaction stage (styrene addition). Thus, two styrene addition reactions (to cation **2a** and to the ion pair **2c**) are characterized by qualitatively different energy profiles. From this standpoint, it is also important to consider an intermediate case (ion pair **2b**).

Styrene addition to **2b** and **2c** proceeds by the same mechanism; however, the energy characteristics of these reactions are appreciably different. Similarly to the reaction with **2c**, the first stage of the reaction with **2b** involves the formation of the intermediate complex **11b** (Figure 5) with a η^1-coordinated benzyl fragment and a η^2-coordinated styrene molecule and requires the overcoming of a much higher energy barrier compared to **2c**. This is due to the presence of two short Ti−F contacts with two F atoms of one of the C_6F_5 rings (2.27 and 2.30 Å, respectively) in **2b**. Only one of these contacts is retained in **11b** (the corresponding distances are 2.36 and 3.74 Å). Thus, a feature of styrene addition to **2b** is a more pronounced weakening of the interaction between the ion pair components than in the case of addition to **2c**. This is also indicated by greater lengthening of the Ti−B distance from 5.25 Å in **2b** to 6.69 Å in **11b**.

Further transformation of **11b** into the pre-reaction complex **7b** via TS **13b** by rotating the styrene molecule in the coordination sphere of Ti requires the overcoming of a low energy barrier (nearly 1.2 kcal mol^{-1}). The energy of TS **13b** is much lower than that of the corresponding TS **13c**. In contrast to **7c**, the formation of **7b** from **11b** is thermodynamically favorable (the energy of the system decreases by 4.5 kcal mol^{-1}). Thus, the energy difference between the barriers **12b**,**c** and **13b**,**c**[25] changes signwise as we pass from $CpTiCH_2$-

Table 4. Thermodynamic Characteristics of Complexes and Transition States 4−10 Relative to the Corresponding Characteristics of Noninteracting Reagents (2 + styrene)

		characteristic			
structure	pathway	ΔE, kcal mol^{-1}	ΔH_0, kcal mol^{-1}	ΔH_{298}, kcal mol^{-1}	ΔG_{298}, kcal mol^{-1}
4a (*2e*)	I − intermediate	−27.8	−26.0	−26.1	−11.7
5a (*3c*)	I − TS	−20.0	−18.0	−18.8	−2.8
6a (*4a*)	I − product 1	−28.5	−25.4	−25.9	−10.8
10a	I − product 2	−42.3	−37.7	−38.7	−21.5
7a	II − intermediate	−29.3	−27.6	−27.6	−13.3
8a	II − TS	−19.4	−16.9	−17.6	−1.7
9a	II − product	−41.9	−37.1	−38.1	−20.9
4b	I − intermediate	−8.6	−6.9	−6.6	6.0
5b	I − TS	1.1	2.7	2.4	16.4
10b	I − product	−23.5	−19.2	−19.7	−5.1
7b	II − intermediate	−9.7	−8.3	−7.9	2.9
8b	II − TS	1.0	3.3	2.9	16.6
9b	II − product	−23.7	−19.1	−19.8	−4.5
4c	I − intermediate	1.4	3.0	3.3	17.9
5c	I − TS	12.1	13.6	13.4	28.7
10c	I − product	−13.0	−8.7	−9.3	7.3
7c	II − intermediate	1.1	2.5	2.9	16.9
8c	II − TS	11.6	13.8	13.5	29.1
9c	II − product	−12.6	−8.1	−8.8	8.2

Scheme 3

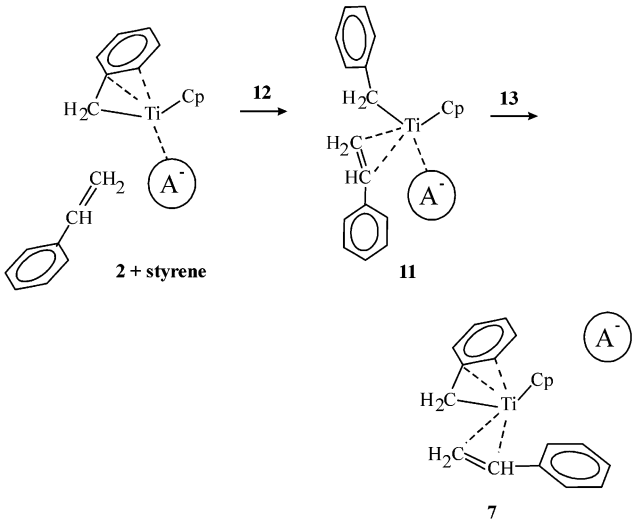

$Ph^+CH_3B(C_6F_5)_3^-$ to the $CpTiCH_2Ph^+B(C_6F_5)_4^-$ ion pair. The results obtained indicate that the styrene addition to $CpTiCH_2Ph^+A^-$ can occur either barrierlessly (in the case of cation **2a**) or with a low energy barrier (in the case of the ion pairs **2b**,**c**), which does not exceed the energy barrier to the C−C bond formation stage. Therefore, the first stage (styrene addition) is not the rate-determining stage of the overall reaction.

III. Transformations of Primary Insertion products $CpTiCH_2CH(Ph)CH_2Ph^+A^-$ (9 and 10). On the basis of the analysis of the structures of the primary interaction products **10a**−**c** and **9a**−**c** for P-I and P-II, respectively, the terminal Ph group in these compounds fills the coordination vacancy of the metal, thus blocking the addition of the next styrene molecule. In this connection, an important question arises as to how the system returns to the beginning of the catalytic cycle (i.e., to its resting state), and what is the role of the counterion in this process.

Similarly to the styrene addition to the resting states **2a**−**c**, further transformations of the insertion product are to a great extent determined by the nature of the counterion A^-. Relaxation of the insertion products **10b**,**c** and **9b**,**c** occurs in a similar way (Scheme 4). Generally, these processes can be described as follows: **10b**,**c** → **14b**,**c** → **15b**,**c** → **16′b**,**c** → **16b**,**c** and **9b**,**c** → **17b**,**c** → **18b**,**c** → **16′b**,**c** → **16b**,**c**, respectively; here **14b**,**c**, **15b**,**c**, **17b**,**c**, and **18b**,**c**[24,25] are the intermediates, and the isomers **16′b**,**c**/**16b**,**c** are β-agostic (**16′b**,**c**), γ-agostic (**16a**,**b**), or nonagostic (**16c**) analogues of the starting complexes **2b**,**c** containing one extra monomer unit. The ways of relaxation of the isolated cations **9a** and **10a** and the ion pairs **9b**,**c** and **10b**,**c** are essentially different. In the former case, relaxation involves one stage (**10a** → **16′a** → **16a** and **9a** → **16′a** → **16a**); it occurs by rotating about the C_1-C_8 bond and leads to an increase in the energy of the system by more than 15 kcal mol^{-1}. In the latter case, the interaction with the counterion in the product (**16′b**,**c**) allows full compensation of the energy losses, although the reaction proceeds in a more complex way (Table 6). Isomers **16′a**−**c** are β-agostic structures. A feature of the complex **16c** (Figure 6) is the absence of agostic bonds, whereas the corresponding complexes **16a**,**b** have two γ-agostic bonds.

Initially, the anion approaches the Ti atom. This is accompanied by a change in hapticity of coordination of the benzyl fragment from η^3 to η^1, while the hapticity of the coordination of the terminal Ph group (η^6) remains unchanged (the formation of intermediates **14b**,**c** and **17b**,**c**, respectively). Further transformations of **14b**,**c** and **17b**,**c** involve elimination of the η^6-Ph fragment from the Ti atom, restoration of η^3-coordination to the $C_9-C_{10}-C_{11}$ atoms lost at the preceding stage, and loss of the η^6-coordination of the Ph group. The relaxation products **15b**,**c** and **18b**,**c** are close analogues of the initial complexes **2b**,**c** (in particular, they also contain η^3-coordinated benzyl fragments). Nevertheless, there are some structural differences between these complexes. For instance, the terminal Ph fragment remains turned toward the Ti ion, thus producing steric hindrances for the next styrene molecule to approach. Complexes **15b**,**c** and **18b**,**c** undergo transformation to

(25) TS **12b** and **13b** and intermediate **17b** are not fully optimized structures; they were located by point-by-point scanning of the PES of the system. Therefore, the estimates of thermodynamic parameters of these structures listed in Tables 5 and 6 should be regarded as rough approximations.

Table 5. Thermodynamic Characteristics of Intermediates 11 and TS 12 and 13 Relative to the Corresponding Characteristics of Noninteracting Reagents (2 + styrene)

structure	structure type	characteristic			
		ΔE, kcal mol^{-1}	ΔH_0, kcal mol^{-1}	ΔH_{298}, kcal mol^{-1}	ΔG_{298}, kcal mol^{-1}
7a	intermediate	−29.3	−27.6	−27.6	−13.3
8a	TS_{ins} (II)	−19.4	−16.9	−17.6	−1.7
11b	intermediate	−5.2	−4.0	−3.5	7.0
12b	TS_{add}	3.0	3.3	3.7	13.6
13b	TS_{isomer}	−4.0	−3.0	−3.0	9.0
7b	intermediate	−9.7	−8.3	−7.9	2.9
8b	TS_{ins} (II)	1.0	3.3	2.9	16.6
11c	intermediate	−4.1	−2.2	−2.0	12.1
12c	TS_{add}	−1.7	−0.9	−0.8	13.1
13c	TS_{isomer}	1.9	3.1	3.0	17.4
7c	intermediate	1.1	2.5	2.9	16.9
8c	TS_{ins} (II)	11.6	13.8	13.5	29.1

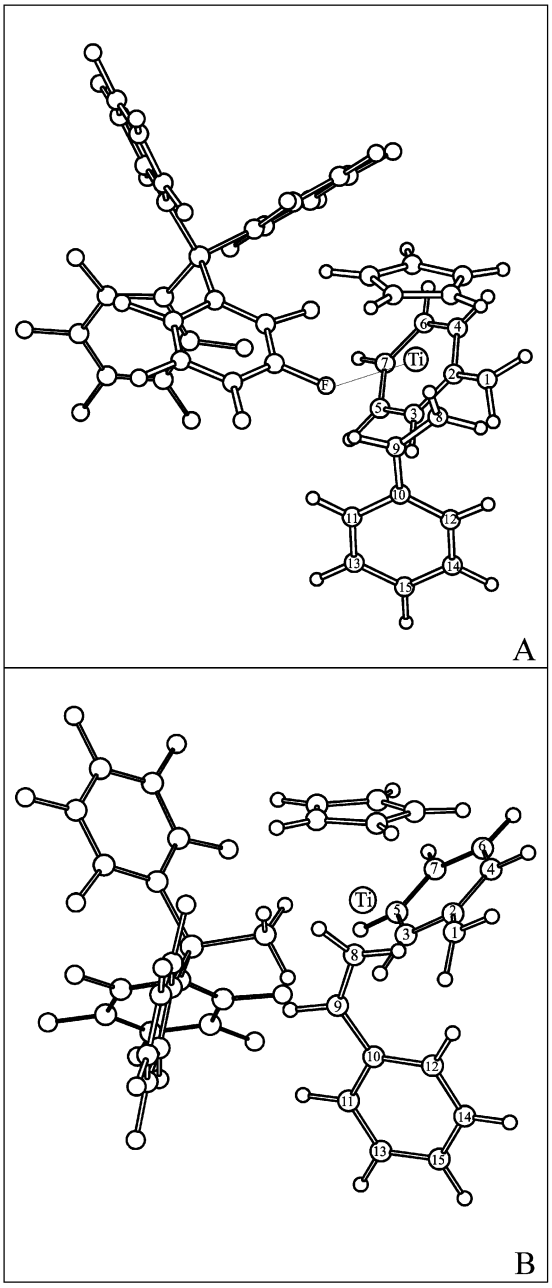

Figure 5. Structures of complexes **11b** (A) and **11c** (B).

the isomers **16′b**,**c** and **16b**,**c** (the analogues of the resting state **2b**,**c**) by rotating about the C_1-C_8 bond.

Complexes **16′a**−**c** undergo a facile transformation into **16a**−**c** by rotating about the C_8-C_9 bond. Thus,

Scheme 4

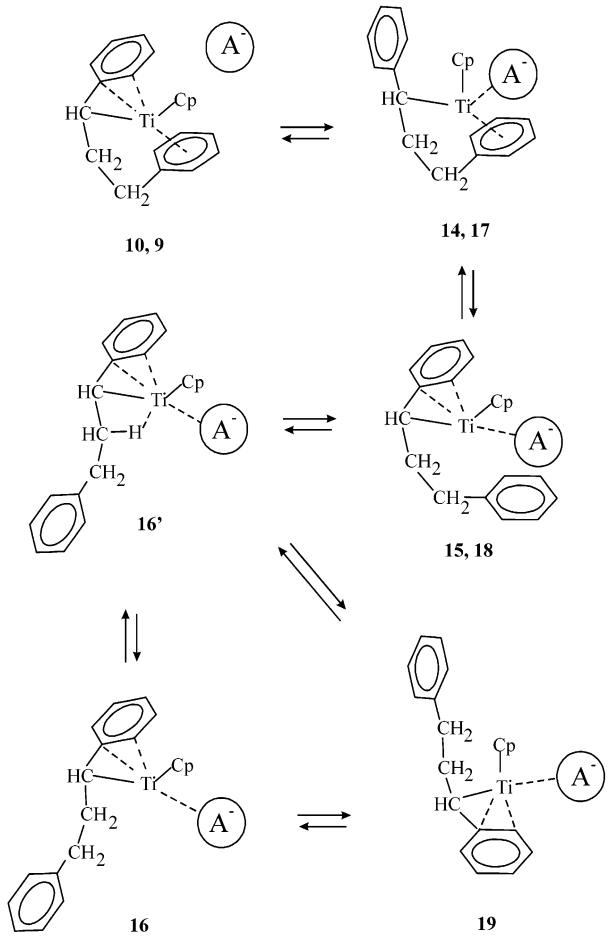

the relaxation of both products, **10a**−**c** (P-I) and **9a**−**c** (P-II), results in the complexes **16a**−**c** and **16′a**−**c**, which can be considered as the analogues of complexes **2a**−**c** with one extra monomer unit.

Complexes **16a**−**c** and **16′a**−**c** can react with the next styrene molecule (by Pathway II) or undergo transformation into nonagostic complexes **19a**−**c**, which are analogues of the initial complexes **2′a**−**c**. In the latter case, further interaction with the styrene molecule proceeds by Pathway I.

Therefore, the role of the counterion at the stage of the relaxation of the primary C−C bond formation product is the compensation of the energy losses arising due to the displacement of the terminal Ph group out of the coordination sphere of the Ti atom. As a result of such compensation, an extremely energetically unfavor-

Table 6. Thermodynamic Characteristics of Complexes 14−19 Relative to Corresponding Noninteracting Reagents (2 + styrene)

		characteristic			
structure	pathway	ΔE, kcal mol^{-1}	ΔH_0, kcal mol^{-1}	ΔH_{298}, kcal mol^{-1}	ΔG_{298}, kcal mol^{-1}
10a	I	−42.3	−37.7	−38.7	−21.5
16′a (β-agostic)	I, II	−25.6	−23.1	−23.4	−10.2
16a (γ-agostic)	I, II	−22.7	−20.0	−20.4	−6.3
9a	II	−41.9	−37.1	−38.1	−20.9
19a	I	−19.8	−17.4	−17.4	−5.3
10b	I	−23.5	−19.2	−19.7	−5.1
14b	I	−14.8	−10.6	−11.2	3.8
15b	I	−14.2	−11.2	−11.4	1.9
16′b (β-agostic)	I, II	−19.9	−16.9	−17.2	−3.6
16b (γ-agostic)	I, II	−9.3	−6.7	−6.6	4.8
9b	II	−23.7	−19.1	−19.8	−4.5
17b	II	−11.4	−7.1	−7.7	7.1
18b	II	−10.5	−7.3	−7.5	5.6
19b	I	−18.8	−16.0	−15.9	−4.4
10c	I	−13.0	−8.7	−9.3	7.3
14c	I	−11.9	−7.7	−8.3	8.9
15c (β-agostic)	I	−15.9	−11.8	−12.1	4.7
16′c (β-agostic)	I, II	−18.3	−8.9	−9.6	6.2
16c	I, II	−16.3	−13.2	−13.4	1.0
9c	II	−12.6	−8.1	−8.8	8.2
17c	II	−9.4	−5.1	−5.7	11.8
18c	II	−10.8	−7.0	−7.4	8.7
19c	I	−18.4	−15.6	−15.7	−1.1

able process in the case of the cation (**10a** → **16′a** → **16a** and **9a** → **16′a** → **16a**) turns into an energetically neutral and even favorable one in the case of the ion pairs (**10b**,**c** → **16′b**,**c** → **16b**,**c** and **9b**,**c** → **16′b**,**c** → **16b**,**c**; see Table 6).

Because the PES at this area is flat, the localization of the transition states presents a grate difficulty. The scanning technique for the energy dependence on the most significant geometric parameters (such as Ti−counterion, Ti−terminal Ph distances, etc.) was employed to estimate the upper limits of the corresponding energy barriers.

The energies of the TS of all transformations mentioned above are at most 5 kcal mol^{-1} for the ion pairs (**b**,**c**). Since the energy difference between the starting compounds (**9b**,**c** and **10b**,**c**) and the products (**16′b**,**c**/**16b**,**c** and **19b**,**c**) is small, this stage must occur with ease under the experimental conditions and cannot be the rate-determining step of the overall process. Therefore, similarly to styrene addition to the initial complexes **2a**−**c**, relaxation of the primary insertion products of styrene into the Ti−C_1 bond (**9a**−**c** and **10a**−**c**) for all the systems studied in this work does not involve the overcoming of energy barriers that are higher than the energy barrier to the C_1−C_8 bond formation stage. Thus, it is this stage that should be considered as the rate-determining step of styrene polymerization on the $CpTiCH_2Ph^+A^-$ ion pairs.

Concluding Remarks

A study of the mechanism and the energy profile of the reaction between the styrene molecule and the model catalytic species $CpTiCH_2Ph^+A^-$, where $A^- = B(C_6F_5)_4^-$ (**b**) or $CH_3B(C_6F_5)_3^-$ (**c**) or no counterion involved (**a**) (Figure 7), suggests that the introduction of the counterion and enhancement of its nucleophilicity (successive passage from **a** to **b** to **c**) lead to a decrease in the exothermicity of styrene coordination with the formation of $CpTi(CH_2CHPh)CH_2Ph^+A^-$ adducts. Earlier,[19] an analogous conclusion was drawn in our study of the reaction $Cp_2ZrEt^+A^- + C_2H_4$ using the same counterions. The results of comparison of the energy profiles of three reactions studied (**a**, **b**, and **c**) suggest that the energy barrier to the C−C bond formation stage is independent of the counterion structure and is a global maximum on the reaction pathway. A diametrically opposite conclusion was drawn in the study of the $Cp_2ZrEt^+A^- + C_2H_4$ system,[19] which was characterized by the presence of the energy barriers to ethylene addition (*TS-1* in ref 19) and to isomerization of the intermediate formed (*TS-2*[19]). The barrier heights were comparable to, or even higher than, the energy barrier to the C−C bond formation (*TS-3*[19]). We believe that these differences in the energy characteristics of two polymerization processes appear to be due to a higher degree of coordinative unsaturation of Ti in $CpTiCH_2Ph^+A^-$ compared to that of Zr in $Cp_2ZrEt^+A^-$ and to lesser steric overcrowding of the former system compared to the latter.

Thus, we have carried out a detailed study of two possible mechanisms of the interaction between the styrene molecule and the $CpTiCH_2Ph^+A^-$ ion pairs taking three systems (**a**, **b**, and **c**) as examples. One mechanism was previously studied by Cavallo et al.[18] taking the isolated cation as an example. This mechanism cannot be directly extended to the ion pairs, since in this case the resting state is η^3-compounds **2b**,**c** (its cationic analogue **2a** was not located earlier[18a]) rather than the η^7-complexes **1b**,**c**. Therefore, Pathway I (P-I) proposed in this work is the modified reaction channel considered in ref 18a extended to the ion pairs case. In addition, we have revealed yet another reaction channel (P-II) involving the formation of different intermediates, TS, and primary reaction products compared to those found for P-I. Since both reaction channels are characterized by similar energy profiles, one can suggest that the reaction can proceed by P-I and P-II nearly equiprobably.

In this work we have shown that the stage of intramolecular formation of the C−C bond in the

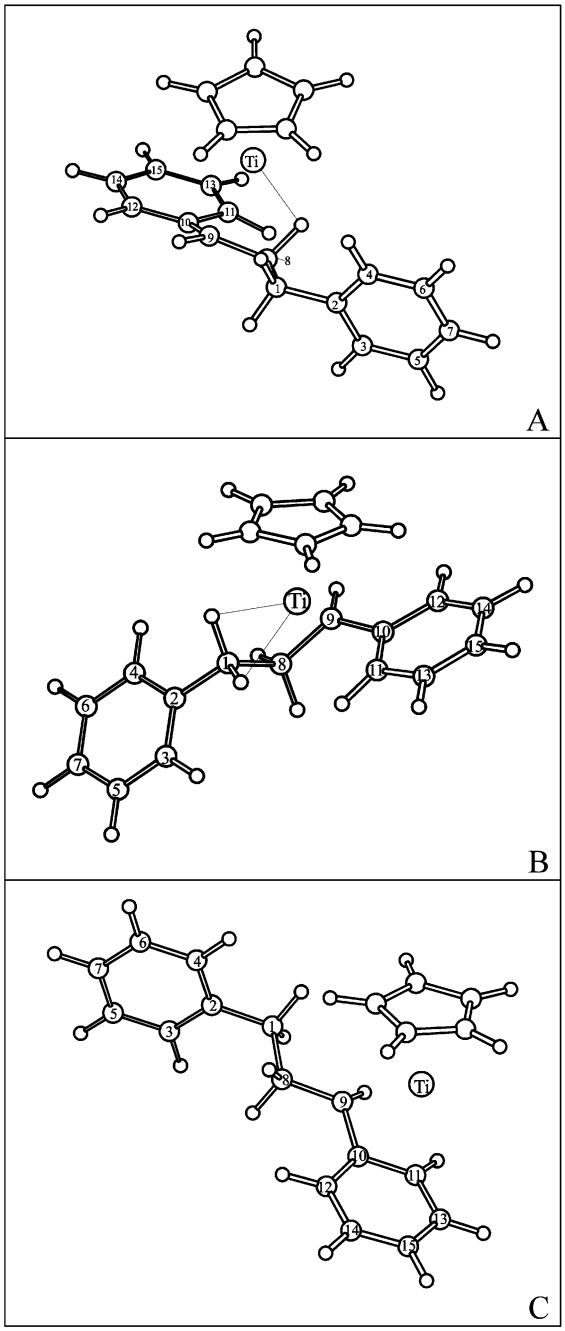

Figure 6. Structures of complexes **16′a** (A), **16a** (B), and **19a** (C).

$CpTi(CH_2CHPh)CH_2Ph^+A^-$ adducts (**4a**−**c** and **7a**−**c** for P-I and P-II, respectively) is characterized by the highest energy on the reaction pathway. In the case of the ion pairs (**b** and **c**) the energy barriers to other reaction stages (styrene addition with the formation of the $CpTi(CH_2CHPh)CH_2Ph^+A^-$ adduct and the relaxation of the primary insertion product $CpTiCH_2CH(Ph)CH_2Ph^+A^-$) are much lower than the energy barrier to the C−C bond formation stage. Therefore, the last-mentioned stage is the rate-determining step of the overall reaction. Relaxation of the primary insertion products **10b**,**c** and **9b**,**c** by P-I and P-II, respectively, is a multistage process involving the formation of several intermediates. It occurs in such a way that the weakening of the interaction with the coordinated terminal Ph group is to the greatest extent compensated by the interaction with the approaching anion.

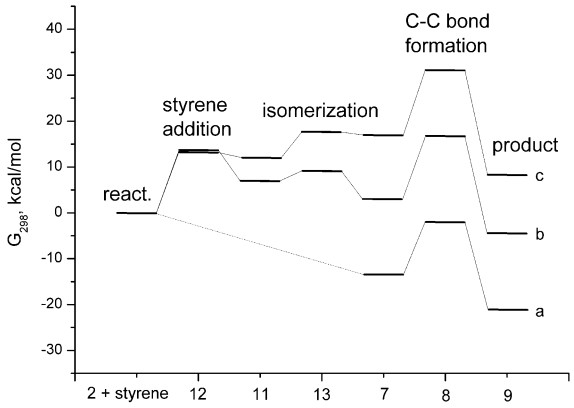

Figure 7. Energy profiles for the transformation **2a**−**c** + styrene → **9a**−**c**.

Therefore, on the basis of our study of the dependence of the interaction between the styrene molecule and the $CpTiCH_2Ph^+A^-$ compounds on the "nucleophilicity" of the counterion, we have drawn qualitative conclusions as to how the energy profile of the reaction changes as the interaction between the components of the ion pair weakens (down to its full absence). Mention should be made as to how the solvation effects could possibly influence the energetics of the process we have considered. While the truthful evaluation of the solvent effect is a challenging task (which, of course, cannot be solved using a conventional procedure based on the continuum models of the medium as it does not take into account the specific interactions between the ion pair and the solvent molecules), we believe that if we were to evaluate this effect, it would lead only to the weakening of the interaction between the ion pair components, as compared to the gas-phase systems. In the other words, in this case, the "loosely bound" ion pair with the $B(C_6F_5)_4^-$ counterion would more resemble the isolated cation, while the "tightly bound" ion pair with the $CH_3B(C_6F_5)_3^-$ counterion would become more "weakly bound"-like. That is, the solvent effects could lead only to slight changes of the quantitative characteristics, but in no way would affect the overall conclusions drawn from our work.

Acknowledgment. Financial support from Basell Polyolefines is gratefully acknowledged. This work was financially supported by RFBR (Project Nos. 02-03-32781, 03-03-06003). The authors express their gratitude to Prof. Yu. A. Ustynyuk and Dr. D. N. Laikov for helpful discussions.

Supporting Information Available: Tables of Cartesian coordinates, gas-phase energies, and thermodynamic data of all DFT-optimized structures and figures of the structures not incorporated in the paper.

OM0300629